

1 Syntrophy via interspecies H₂ transfer between *Christensenella* and
2 *Methanobrevibacter* underlies their global co-occurrence in the human gut

3

4 Albane Ruaud^a, Sofia Esquivel-Elizondo^{a,b}, Jacobo de la Cuesta-Zuluaga^a, Jillian L.
5 Waters^a, Largus T. Angenent^b, Nicholas D. Youngblut^a, Ruth E. Ley^{a#}

6

7 ^a Department of Microbiome Science, Max Planck Institute for Developmental Biology,
8 Germany.

9 ^b Center for Applied Geosciences, Eberhard-Karls-Universität Tübingen, Germany.

10

11 Running head: H₂ transfer between *Christensenella* and *M. smithii*

12

13 #Address correspondence: rley@tuebingen.mpg.de

14

15 Albane Ruaud and Sofia Esquivel-Elizondo contributed equally to this work. Author
16 order was determined on the basis of substantial relative contribution differences.

17

18 Abstract word count: 219

19 Importance word count: 150

20 Text word count: 5,724

21

22

23 **Abstract**

24 Across human populations, 16S rRNA gene-based surveys of gut microbiomes
25 have revealed that the bacterial family *Christensenellaceae* and the archaeal family
26 *Methanobacteriaceae* co-occur and are enriched in individuals with a lean, compared to
27 an obese, BMI. Whether these association patterns reflect interactions between
28 metabolic partners remains to be ascertained, as well as whether these associations
29 play a role in the lean host phenotype with which they associate. Here, we validated
30 previously reported co-occurrence patterns of the two families, and their association
31 with a lean BMI, with a meta-analysis of 1,821 metagenomes derived from 10
32 independent studies. Furthermore, we report positive associations at the genus and
33 species level between *Christensenella* spp. and *Methanobrevibacter smithii*, the most
34 abundant methanogen of the human gut. By co-culturing three *Christensenella* spp. with
35 *M. smithii*, we show that *Christensenella* spp. efficiently support the metabolism of *M.*
36 *smithii* via H₂ production, far better than *Bacteroides thetaiotaomicron*. *C. minuta* forms
37 flocs colonized by *M. smithii* even when H₂ is in excess. In culture with *C. minuta*, H₂
38 consumption by *M. smithii* shifts the metabolic output of *C. minuta*'s fermentation
39 towards acetate rather than butyrate. Together, these results indicate that the
40 widespread co-occurrence of these microbiota is underpinned by both physical and
41 metabolic interactions. Their combined metabolic activity may provide insights into their
42 association with a lean host BMI.

43

44

45

46 **Importance**

47 The human gut microbiome is made of trillions of microbial cells, most of which
48 are *Bacteria*, with a subset of *Archaea*. The bacterial family *Christensenellaceae* and
49 the archaeal family *Methanobacteriaceae* are widespread in human guts. They correlate
50 with each other and with a lean body type. Whether species of these two families
51 interact, and how they affect the body type, are unanswered questions. Here, we
52 showed that species within these families correlate with each other across people. We
53 also demonstrated that particular species of these two families grow together in dense
54 flocs, wherein the bacteria provide hydrogen gas to the archaea, which then make
55 methane. When the archaea are present, the ratio of bacterial products (which are
56 nutrients for humans) is changed. These observations indicate when these species
57 grow together, their products have the potential to affect the physiology of their human
58 host.

59 Introduction

60 Obesity was the first human disease phenotype to be associated with an altered
61 microbial ecology of the gut (1, 2). The link between the relative abundance in the gut of
62 the bacterial family *Christensenellaceae* and a low host body mass index (BMI) now
63 stands as one of the most robust associations described between the human gut
64 microbiome and host BMI (3–15). Compared to other families of bacteria that comprise
65 the human gut microbiome, the family *Christensenellaceae* was described relatively
66 recently, when the type strain *Christensenella minuta* was reported in 2012 (16). Prior to
67 the description of *C. minuta*, 16S rRNA sequences from this genus escaped notice in
68 the gut microbiome, though these sequences accumulated steadily in SSU rRNA gene
69 databases. A positive association between a lean host BMI and the relative abundance
70 in the gut of *Christensenellaceae* 16S rRNA genes was first reported in 2014 (4). The
71 association was shown to have existed in earlier datasets (4), but was likely undetected
72 as this family had not yet been named. Goodrich *et al.* showed a causal link between
73 the *Christensenellaceae* and host BMI in gnotobiotic mice: the addition of *C. minuta* to the
74 gut microbiome of an obese human donor prior to transplantation reduced adiposity
75 gains in the recipient mice compared to controls receiving the unsupplemented
76 microbiome (4). The mechanism underlying this host response remains to be
77 elucidated. One step towards this goal is a better understanding of how the members of
78 the *Christensenellaceae* interact ecologically with other members of the gut microbiome.

79 Across human populations, gut microbiota often form patterns of co-occurrence
80 (*e.g.*, when these consortia exist in a subset of human subjects, they are termed enterotypes
81 (17)). Such co-occurrences of taxa across subjects reflect shared environmental

82 preferences, but to determine if they represent metabolic or physical interactions
83 requires further study. The family *Christensenellaceae* consistently forms the hub of co-
84 occurrence networks with other taxa (6, 8, 9, 18, 19). Notably, gut methanogens
85 (specifically, of the archaeal family *Methanobacteriaceae*) are often reported as part of
86 the *Christensenellaceae* co-occurrence consortium (4, 20–22). The most widespread
87 and abundant of the gut methanogens, *Methanobrevibacter smithii*, produces CH₄ from
88 H₂ and CO₂, the products of bacterial fermentation of dietary fibers. Such cross-feeding
89 likely explains why the relative abundances of *M. smithii* and fermenting bacteria are
90 often positively correlated (21, 23, 24). Several studies have shown that in the
91 laboratory, *M. smithii* can grow from the H₂ provided by *Bacteroides thetaiotaomicron*, a
92 common gut commensal bacterium (25–27). Given that the cultured representatives of
93 the *Christensenellaceae* ferment simple sugars (16, 28), and that their genomes
94 contains hydrogenases (29), we predicted that members of the *Christensenellaceae*
95 produce H₂ used by *M. smithii* as a substrate in methanogenesis.

96 Here, we explored the association between the *Christensenellaceae* and the
97 *Methanobacteriaceae* in two ways. First, we analyzed metagenomes for statistical
98 associations between the two families and their subtaxa. Compared to 16S rRNA gene
99 surveys, metagenomes often can better resolve the taxonomic assignments of
100 sequence reads below the genus level (30). Metagenome-based studies have so far
101 been blind to the *Christensenellaceae*, however, because their genomes have been
102 lacking from reference databases. Here, we customized a reference database to include
103 *Christensenellaceae* genomes, which we used in a meta-analysis of >1,800
104 metagenomes from 10 studies. Second, to assess for metabolic interactions between

105 members of the *Christensenellaceae* and *Methanobacteriaceae*, we measured methane
106 production by *M. smithii* when grown in co-culture with *Christensenella* spp. Our results
107 show that: i) the positive association between the *Christensenellaceae* and the
108 *Methanobacteriaceae* is robust to the genus/species level across multiple studies; ii)
109 these taxa associate with a lean host BMI; iii) *Christensenella* spp. support the growth of
110 *M. smithii* by interspecies H₂ transfer far better than *B. thetaiotaomicron*; and iv) *M.*
111 *smithii* directs the metabolic output of *C. minuta* towards less butyrate and more acetate
112 and H₂, which is consistent with reduced energy availability to the host and consistent
113 with the association with a low BMI.

114

115 **Results**

116 ***Christensenella* relative abundance is significantly correlated with leanness**
117 **across populations** - Both the *Christensenellaceae* family and the genus
118 *Christensenella* had a very high prevalence, as they were present in more than 99% of
119 the 1,821 samples; both the family and the genus have a mean abundance of 0.07% ±
120 0.05 (Fig. 1b,d and Fig. S1). To correct for the influence of environmental factors on the
121 relative abundance of the *Christensenellaceae* family and of the *Christensenella* genus,
122 we first constructed null models in which we selected covariates (Appendix 1) that
123 explained a significant proportion of the variance of the transformed relative abundance
124 of the family *Christensenellaceae*, and in the same manner of the *Christensenella*
125 genus. BMI and age were significantly correlated to the transformed relative

126 abundances of *Christensenellaceae* and of *Christensenella* (designated with the suffix ‘-
127 tra’, i.e., Cf-tra and Cg-tra), and were retained in the null models (Cf-null and Cg-null).

128 BMI was negatively correlated to both Cf-tra (type II ANOVA, p-value = 0.0002
129 and F-value(339) = 14.46) and Cg-tra (type II ANOVA, p-value = 0.0002 and F-
130 value(339) = 14.29), indicating that leaner individuals harbor higher relative abundances
131 of *Christensenellaceae* and *Christensenella*. Age was negatively correlated with Cf-tra
132 (type II ANOVA, p-value = 0.01 and F-value(1,468) = 6.56) and with Cg-tra (type II
133 ANOVA, p-value = 0.01 and F-value(1,468) = 6.53), indicating that younger subjects
134 carry a greater relative abundance of *Christensenellaceae* and *Christensenella*. However,
135 the interaction term between BMI and age was not significantly correlated to the
136 transformed relative abundances (type II ANOVA, p-values > 0.1), indicating that their
137 effects are additive. These results show that regardless of their BMI, younger subjects
138 have higher levels of *Christensenellaceae* and *Christensenella*, and that the lower a
139 subject’s BMI, the more of these microbes they harbor, regardless of their age.

140

141 ***Methanobrevibacter* relative abundance is significantly correlated with**
142 **leanness across populations** - The *Methanobacteriaceae* family and
143 *Methanobrevibacter* genus also had a high prevalence with 92% and 89% of the people
144 harboring them respectively, with mean abundances of 0.48% ± 1.55 and 0.49% ± 1.54,
145 respectively. As above, we evaluated the association between the
146 *Methanobacteriaceae* family, and of the *Methanobrevibacter* genus, with BMI and age
147 (models Mf-null and Mg-null). The transformed relative abundances of
148 *Methanobacteriaceae*, Mf-tra, and of *Methanobrevibacter*, Mg-tra, were also negatively

149 correlated to BMI (type II ANOVA, respective p-values = 0.01 and 0.02, F-values(341;
150 341) = 6.66 and 5.11). In contrast to the *Christensenellaceae*, both
151 *Methanobacteriaceae* and *Methanobrevibacter* were positively correlated with age (type
152 II ANOVA, respective p-values = 0.001 and 4.27×10^{-4} , F-values(1,468; 1,468) = 10.35
153 and 12.47), indicating that older people carry a greater proportion of methanogens.
154 Moreover, *M. smithii*, the most abundant and prevalent methanogen species within the
155 human gut, was also positively correlated with age and negatively with BMI regardless
156 of age, *i.e.* the interaction term between age and BMI was not significantly correlated
157 (Appendix 2, additional statistics).

158

159 **The relative abundances of the *Christensenella* and *Methanobrevibacter***
160 **genera are significantly correlated across populations** - Next, we looked into how
161 the *Christensenellaceae* and the *Methanobacteriaceae* correlated with each other
162 across subjects while controlling for BMI and age. We constructed a model where Mf-tra
163 was included in addition to BMI and age (model Cf-Mf). This allowed us to test whether
164 adding Mf-tra to the model improved its fit and if so, how much of the variance of Cf-tra
165 not explained by age and BMI could be explained by Mf-tra. We also evaluated the
166 interaction terms between Mf-tra and BMI, and between Mf-tra and age, to assess
167 whether the correlation between Cf-tra and Mf-tra was dependent on age and BMI. The
168 interaction term for BMI and Mf-tra was not significant and was removed from the
169 model; the interaction term for age and Mf-tra was significant and was retained (type I
170 ANOVA, F-value(339) = 8.30 and p-value = 0.0042). We compared the log-likelihoods
171 of the null and full models (Cf-null and Cf-Mf) to confirm that the relative abundances of

172 the *Methanobacteriaceae* and *Christensenellaceae* families were significantly correlated
173 (χ^2 test, p-value = 1.78×10^{-59}). Furthermore, the model Cf-Mf showed that Mf-tra was
174 significantly positively correlated to Cf-tra (Fig. 1b; type I ANOVA, F-value(339) =
175 287.03, p-value < 0.0001) and that the interaction term between Mf-tra and age was
176 positively correlated to Cf-tra as well. These results indicate that the relative
177 abundances of the *Christensenellaceae* and *Methanobacteriaceae* families are
178 positively correlated across multiple populations/studies. In addition, although both
179 families are enriched in low-BMI people, they are correlated regardless of a subject's
180 BMI. Moreover, their association is stronger in older people, suggesting that although
181 elders are less likely to carry as much *Christensenellaceae* as youths, the more
182 *Methanobacteriaceae* they have, the more *Christensenellaceae* they have.

183 We performed a similar analysis using the abundances of the two most
184 prominent genera belonging to these families (*Christensenella* and *Methanobrevibacter*,
185 models Cg-null and Cg-Mg) and obtained equivalent results. First, the interaction term
186 between Mg-tra and age was positively correlated with Cg-tra (Fig. 1c; type I ANOVA,
187 F-value(339) = 10.19, p-value = 0.0015). Then, by comparing model Cg-null with the full
188 model Cg-Mg, we showed that the relative abundances of the two genera were also
189 correlated (χ^2 test, p-value = 1.50×10^{-57}). Our full model Cg-Mg showed that Mg-tra was
190 significant for predicting Cg-tra while controlling for BMI and age (type I ANOVA, F-
191 value(339) = 274.35, p-value < 0.0001), with the interaction term between Mg-tra and
192 age also positively correlated to Cg-tra. These results indicate that the correlations
193 between the relative abundances of the two families, explained above, hold true at the

194 level of two representative genera. The association between *Methanobrevibacter* and
195 *Christensenella* is stronger in older people regardless of BMI.

196 A similar analysis at the species level indicated that *C. minuta* and *M. smithii*
197 were the most abundant species of each of their genera, and similarly to the family and
198 genus ranks, their relative abundances across samples were significantly correlated
199 (Fig. 1d and Appendix 2). The less abundant *Christensenella* gut species, *C.*
200 *massiliensis* and *C. timonensis*, also correlated with *Methanobrevibacter smithii* across
201 the 1,821 metagenomes (Appendix 2). *C. minuta* and *C. timonensis* transformed relative
202 abundances were significantly negatively correlated to both BMI and age, while *C.*
203 *massiliensis* transformed relative abundance was significantly correlated with BMI but
204 not with age. Leaner people are thus enriched in members of the *Christensenellaceae*
205 family, and *C. minuta* and *C. timonensis* are more abundant in younger people than in
206 older people.

207

208 ***C. minuta* forms flocs alone and in co-culture with *M. smithii*** - To assess the
209 physical and metabolic interaction of two representative species, we used *C. minuta*
210 DSM-22607, previously shown to reduce adiposity in germfree mouse fecal transplant
211 experiments (4), and *M. smithii* DSM-861, which is the most abundant and prevalent
212 methanogen in the human gut (31). Confocal and scanning electron imaging of 2-7 day-
213 old cultures revealed that *C. minuta* flocculate in mono- and co-cultures (Fig. 2a,b and
214 Fig. 3a-c, g-j). *M. smithii* is present within the *C. minuta* flocs (Fig. 2d and Fig. 3g-j) but
215 does not aggregate in mono-culture before 7-10 days of culture (data not shown). In
216 contrast, *B. thetaiotaomicron*, used here as a positive control based on previous reports

217 that it supports the growth of *M. smithii* via H₂ production (25, 26), did not flocculate
218 when grown alone, (Fig. 2c) and, when co-cultured with *M. smithii*, displayed very
219 limited aggregation (Fig. 2e, Fig. 3k-n and Fig. S2).

220

221 **H₂ and CH₄ production** - After 6 days in mono-culture, *C. minuta* had produced
222 7 times more H₂ than *B. thetaiotaomicron* (14.2 ± 1.6 mmol.L⁻¹ vs. 2.0 ± 0.0 mmol.L⁻¹,
223 Fig. 4a and d and Fig. 5a; Wilcoxon rank sum test, p-value = 0.1). As expected, *M.*
224 *smithii* did not grow in mono-culture when H₂ was not supplied (80:20 % v/v N₂:CO₂
225 headspace, Fig. 4b). After 6 days, *M. smithii* had produced 9.0 ± 1.0 mmol.L⁻¹ of CH₄
226 when H₂ was provided in excess (*i.e.*, 80:20 % v/v H₂:CO₂ atmosphere at 2 bars; Fig. 4b
227 and Fig. 5b).

228 In accordance with the higher levels of H₂ produced by *C. minuta* compared to *B.*
229 *thetaitaomicron*, day-6 CH₄ concentrations were higher for *M. smithii* co-cultured with
230 *C. minuta* compared to with *B. thetaiotaomicron* (respectively 5.8 ± 0.5 mmol.L⁻¹ and
231 1.1 ± 0.0 mmol.L⁻¹; Wilcoxon rank sum test, p-value = 0.1; Fig. 4c and e and Fig. 5b).

232 For both co-culture conditions, H₂ concentrations were very low (on average across time
233 points and replicates, H₂ concentrations were 0.5 ± 0.6 mmol.L⁻¹ in co-cultures with *C.*
234 *minuta*, and 0.1 ± 0.1 mmol.L⁻¹ with *B. thetaiotaomicron*), indicating that almost all the
235 H₂ that had been produced was also consumed (Fig. 4c and e and Fig. 5a).

236

237 **Pressure effects on gas production and aggregation - Gas consuming**
238 microbes, including hydrogenotrophic methanogens, grow better in a pressurized
239 environment (32–34) due to a higher gas solubility at higher pressure, as described by
240 Henry's law. We compared CH₄ production by *M. smithii* in mono-culture and in co-
241 culture with *C. minuta* under 2 different pressures (*i.e.*, 2 bar and atmospheric
242 pressure). Similar to the flocculation at 2 bar (Fig. 2d), *C. minuta* and *M. smithii* also
243 aggregated at atmospheric pressure (Fig. S3a-b). Accordingly, *C. minuta* supported
244 CH₄ production by *M. smithii* to a similar extent under both pressure conditions (ANOVA
245 followed by Tukey's post-hoc test, adjusted p-value = 1.0; Fig. 4c, Fig. 5b and, even
246 though the putative H₂ produced by *C. minuta* (estimated based on the mono-cultures)
247 was much lower than the amount of H₂ provided in the headspace for *M. smithii* (Fig.
248 5a).

249 We next sought to assess if the mixed aggregation of *M. smithii* with *C. minuta*
250 could be disrupted if H₂ was pressurized in the medium, reducing *M. smithii*'s reliance
251 on *C. minuta* as a H₂ source. We observed that *M. smithii* aggregated with *C. minuta*
252 (Fig. S3c-d) even though H₂ was abundant. Total CH₄ production was higher than in
253 mono-culture under the same headspace, reaching 14.2 ± 5.3 mmol.L⁻¹ in co-culture vs.
254 9.0 ± 1.0 mmol.L⁻¹ in mono-culture after 6 days (ANOVA followed by Tukey's post-hoc
255 test, adjusted p-value = 0.1, Fig. 4b and c). This indicates that interspecies H₂ transfer
256 occurs even when H₂ is added to the headspace, and leads to greater methanogenesis.

257

258 **The short chain fatty acid (SCFA) production of *C. minuta* is influenced by**

259 **the presence of *M. smithii*** - Regardless of headspace composition and pressure
260 conditions, the only SCFAs detected as produced by *C. minuta* in mono-culture were
261 acetate and butyrate (among 10 short and medium chain fatty acids analyzed, Appendix
262 1; Fig. 5). To investigate if the consumption of H₂ by *M. smithii* influenced the SCFA
263 production profile of *C. minuta*, we compared acetate and butyrate concentrations
264 between the co-cultures and *C. minuta*'s mono-cultures under all conditions tested (*i.e.*,
265 cultures at 2 bar or atmospheric pressure with an 80:20 % v/v N₂:CO₂ or H₂:CO₂
266 headspace, Table S1).

267 We consistently observed lower butyrate concentrations in all co-cultures
268 compared to mono-cultures (Fig. 6a-c, Fig. 5c; ANOVA, F-value(1) = 161.461 and
269 adjusted p-value = 7.7x10⁻⁸). For all conditions, butyrate concentrations in co-culture
270 after 6 days were 1.1 ± 0.24 mmol.L⁻¹ lower than in mono-cultures (Fig. 6a-c and Table
271 A3). The interaction factor between the mono/co-culture conditions and the growth
272 condition was not significantly correlated to butyrate concentrations (ANOVA, F-value(2)
273 = 0.862, adjusted p-value = 0.4). The observation that butyrate concentrations in co-
274 cultures were lower than in mono-cultures regardless of pressure and headspace
275 composition suggest that the methanogen's presence shapes the metabolite output of
276 *C. minuta*.

277 Along with the reduced butyrate production, we also observed slightly but
278 significantly higher acetate production in co-cultures compared to mono-cultures (Fig.
279 6d-f, Fig. 5d; ANOVA, F-value(1) = 317.41 and adjusted p-value = 3.2x10⁻⁹). This
280 difference was also observed in three additional batches performed at 2 bars (Fig. S4).

281 The difference in acetate production between mono and co-culture conditions
282 significantly varied with the headspace and pressure conditions (interaction term
283 between the mono- or co-culture and the growth condition was significantly correlated to
284 acetate production; ANOVA, F-value(2) = 29.09 and adjusted p-value = 3.0×10^{-5}). The
285 differences in final acetate production (after 6 days) ranged from $+0.7 \text{ mmol.L}^{-1}$ at 2 bar
286 under an $\text{H}_2:\text{CO}_2$ (80:20 % v/v) atmosphere to $+2.2 \text{ mmol.L}^{-1}$ at atmospheric pressure
287 under an $\text{N}_2:\text{CO}_2$ (80:20 % v/v) atmosphere. Furthermore, we observed in co-culture
288 more CH_4 than what *M. smithii* could have produced based on the H_2 production in *C.*
289 *minuta*'s mono-cultures (Appendix 3). This observation implies that *C. minuta* likely
290 produced a greater amount of H_2 in the co-cultures along with greater acetate
291 production.

292

293 ***C. massiliensis* and *C. timonensis* also support the metabolism of *M.***

294 ***smithii*** - We performed similar co-culture experiments of *M. smithii* with *C. massiliensis*
295 and *C. timonensis* at atmospheric pressure. *C. massiliensis* and *C. timonensis*
296 aggregated in mono-culture, and *M. smithii* grew within their flocs in co-culture (Fig. 7).
297 The H_2 produced by the bacteria in mono-culture after 6 days of growth (6.9 ± 0.5
298 mmol.L^{-1} for *C. massiliensis* and $0.6 \pm 0.1 \text{ mmol.L}^{-1}$ for *C. timonensis*, Fig. 8a,d) was
299 lower than the levels produced by *C. minuta* (Fig. 4a). CH_4 production in the co-cultures
300 reached $4.0 \pm 0.2 \text{ mmol.L}^{-1}$ with *C. massiliensis* and $1.5 \pm 0.3 \text{ mmol.L}^{-1}$ with *C.*
301 *timonensis*. These amounts of methane are significantly lower than what we observed

302 for *M. smithii* with *C. minuta* (6.6 ± 0.8 mmol.L⁻¹; ANOVA followed by a Tukey's post-
303 hoc test, adjusted p-values = 6.8×10^{-2} and 1.7×10^{-3} for co-cultures respectively with *C.*
304 *massiliensis* and *C. timonensis* against *C. minuta*; Fig. 8c,e, and Fig. 4c).

305 We observed less butyrate production in the co-cultures compared to mono-
306 cultures (Wilcoxon rank sum test, p-values = 0.33 for *C. massiliensis* and 0.5 for *C.*
307 *timonensis*; Fig. 8f,g), with butyrate measured barely above the detection limit in co-
308 cultures. While in mono-cultures, *C. massiliensis* and *C. timonensis* produced $0.93 \pm$
309 0.06 mmol.L⁻¹ and 1.10 ± 0.00 mmol.L⁻¹ of butyrate, respectively; in co-culture with *M.*
310 *smithii* they produced 0.20 ± 0.14 mmol.L⁻¹ and 0.13 ± 0.15 mmol.L⁻¹, respectively.

311 Acetate production by *C. massiliensis* was higher in co-culture compared to mono-
312 culture (7.83 ± 0.49 mmol.L⁻¹ of acetate produced in mono-culture by day 6 and $9.75 \pm$
313 0.78 mmol.L⁻¹ produced in co-culture with *M. smithii*), although this difference was not
314 significant (Wilcoxon rank sum test, p-value = 0.2). And in contrast with the co-cultures
315 of *C. minuta* with *M. smithii*, acetate production by *C. timonensis* was not higher in the
316 co-cultures compared to mono-cultures: *C. timonensis* produced 5.05 ± 0.21 mmol.L⁻¹
317 in mono-culture and 4.33 ± 1.21 mmol.L⁻¹ in co-culture (Wilcoxon rank sum test, p-value
318 = 0.8; Fig. 8h,i).

319

320 **Discussion**

321 The link between the relative abundance of the *Christensenellaceae* and host
322 BMI now stands as one of the most reproducible associations described between the
323 gut microbiome and obesity (4–15). Here, we confirm in a meta-analysis of
324 metagenomes across 10 populations, the previously observed association between
325 leanness and the *Christensenellaceae* family (4, 20–22). We could also show that
326 *Christensenella* genus and *Christensenella* spp. also correlated with leanness. Similarly,
327 we observed correlations between leanness and the *Methanobacteriaceae* family, the
328 *Methanobrevibacter* genus and *M. smithii*. These methanogens were positively
329 correlated with members of the *Christensenellaceae* family. The relative abundances of
330 the *Christensenellaceae* were higher in young people, whereas conversely,
331 *Methanobacteriaceae* was enriched in older people. Despite these opposite patterns,
332 the two families correlate with each other regardless of age and BMI.

333 We selected the two most prominent members of the two families, *C. minuta* and
334 *M. smithii*, to ask if physical and metabolic interactions could underlie these positive
335 associations. *C. minuta* produced copious amounts of H₂ during fermentation. In co-
336 culture with *C. minuta*, *M. smithii* produced comparable amounts of CH₄ as in mono-
337 culture with an excess of H₂, indicating that *C. minuta* can efficiently support the growth
338 of *M. smithii* via interspecies H₂ transfer. *C. minuta* formed flocs visible by eye, and *M.*
339 *smithii* grew within these flocs.

340 *M. smithii* would likely benefit by associating with the flocs formed by *C. minuta*
341 through better access to H₂. Interspecies metabolite transfer corresponds to the

342 diffusion of a metabolite (e.g., H₂) from the producer (e.g., *C. minuta*) to the consumer
343 (e.g., *M. smithii*). As described by Fick's law of diffusion, the flux of a metabolite
344 between two microorganisms is directly proportional to the concentration gradient and
345 inversely proportional to the distance, such that the closer the microorganisms are, the
346 better the H₂ transfer (35, 36). Thus, within the flocs the H₂ interspecies transfer would
347 be more efficient, to the benefit of *M. smithii*. In accord, we observed greater methane
348 production under excess H₂ when *C. minuta* was present.

349 When grown in co-culture, *M. smithii* influenced the metabolism of *C. minuta*. The
350 presence of the methanogen inhibited the production of butyrate while enhancing
351 acetate production by *C. minuta* under all growth conditions, on average among all
352 experimental batches. This observation suggests that H₂ consumption by *M. smithii*
353 decreased the P_{H₂} within the floc enough to favor acetate production (37). The
354 consumption of H₂ causes the cell to produce more oxidized fermentation products such
355 as acetate (38–41), and the interspecies H₂ transfer leads to greater CH₄ production.

356 Both the methane production and the co-flocculation were far more pronounced
357 when *M. smithii* was grown with *C. minuta* compared to with *B. thetaiotaomicron*. *B.*
358 *thetaiotaomicron* has previously been shown to support the growth of *M. smithii* in co-
359 culture (25, 26). *B. thetaiotaomicron* barely aggregated, in contrast to *C. minuta*'s very
360 large (visible to the naked eye) flocs. When grown together, *B. thetaiotaomicron* and *M.*
361 *smithii* showed very poor aggregation. Moreover, acetate was the only SCFA detected
362 in mono-cultures of *B. thetaiotaomicron*, and its production was less affected by the
363 methanogen compared to *C. minuta*. Methane produced by *M. smithii* in co-culture with
364 *B. thetaiotaomicron* was one fifth of that produced with *C. minuta*, possibly as a result of

365 the smaller amount of H₂ produced and the reduced contact between cells. Given that
366 *M. smithii* does not co-occur with *B. thetaiotaomicron* in human microbiome datasets,
367 this is another indication that co-occurrence patterns may point to metabolic
368 interactions.

369 *C. massiliensis* and *C. timonensis* also produced H₂, acetate and butyrate, and
370 also flocculated in mono-culture. *C. massiliensis* and *C. timonensis* supported methane
371 production by *M. smithii*, which grew within the bacterial flocs. However, *M. smithii* also
372 grew outside the flocs when co-cultured with these two species, which we did not
373 observe in the co-cultures with *C. minuta*. And although *M. smithii* also influenced
374 fermentation of *C. massiliensis* and *C. timonensis*, the overall changes in SCFA
375 production in co-culture were different from what we observed with *C. minuta*: butyrate
376 production was almost undetectable, while acetate production was not significantly
377 affected.

378 These results suggest that the interaction between *M. smithii* and *C. minuta*
379 leads to higher methane production compared to *B. thetaiotaomicron* and to other
380 species of the *Christensenellaceae*, possibly due to the higher levels of interspecies H₂
381 transfer. Nevertheless, *C. massiliensis* and *C. timonensis* did support CH₄ production
382 better compared to *B. thetaiotaomicron*. The higher H₂ production of *C. massiliensis*
383 compared to *B. thetaiotaomicron* might explain this. In the case of *C. timonensis*,
384 although it produced half of the H₂ produced by *B. thetaiotaomicron* in mono-culture, *M.*
385 *smithii* produced more CH₄ in co-culture with *C. timonensis* than with *B.*
386 *thetaitaomicron*. This suggests that, similar to its effect on *C. minuta*, *M. smithii* also
387 triggered the production of H₂ by *C. timonensis*.

388 Altogether, our work demonstrates that members of the *Christensenellaceae* act
389 as a H₂ source to methanogens, and this process is enhanced via close physical
390 proximity. Such interactions also likely underlie the co-occurrence patterns of the
391 *Christensenellaceae* with other members of the microbiome. Many of these families lack
392 cultured representatives, such as the *Firmicutes* unclassified SHA-98, *Tenericutes*
393 unclassified RF39 and unclassified ML615J-28 (4). Based on our results, cultivation of
394 these elusive members of the microbiome may require H₂ (or the provision of another
395 metabolite that *C. minuta* produces when H₂ is being consumed). Despite their very low
396 abundance in the human gut, members of the *Christensenellaceae* may shape the
397 composition of the gut microbiome by favoring the colonization and persistence of
398 certain hydrogenotrophs, and by supplying other butyrate producers with acetate (42).

399 Here, we confirmed an association of *M. smithii* and leanness based on
400 metagenomes from 10 studies. In contrast, some studies have reported an association
401 between *M. smithii* and obesity (2, 43). In this scenario, H₂ uptake by *M. smithii* would
402 promote the breakdown of non-digestible carbon sources by fermenters, such as
403 acetogens, thereby increasing the amount of acetate or other SCFA that can be
404 absorbed and utilized by the host and promoting fat storage (2, 44). In contrast, and
405 consistent with our results, *M. smithii* has also been repeatedly associated with anorexia
406 and leanness (4, 45–48). In this case, the production of CH₄ would decrease the
407 amount of energy available for the host via carbon loss, as has been observed in
408 livestock (49–52). Thus our observation, that the presence of *M. smithii* directs the
409 metabolic output of the *C. minuta* towards greater H₂ availability for methanogenesis,
410 via increased acetate production, is consistent with their association with a lean

411 phenotype. To assess quantitatively how the presence and activity of these microbes
412 impact host physiology will require careful modeling of energy flow *in-vivo*.

413

414 **Materials and methods**

415 **Metagenome data generation** - We generated 141 metagenomes from fecal
416 samples obtained as part of a previous study (53) (Supplementary Table S2).

417 Metagenomic libraries were prepared as described in Appendix 1, Additional methods.

418 **Data from public databases** - We constructed a metagenome sequence
419 collection from: i) the newly generated data (above) to complement the 146
420 metagenomes previously reported in Poole et al., 2019 (53); and ii) publicly available
421 shotgun-metagenome sequences from stool samples included in the
422 curatedMetagenomicData package of Bioconductor (54) for which BMI information was
423 provided. For the latter, we restricted our analyses to individuals for which the following
424 information was available: gender, age, country of origin, and BMI. Individuals with
425 *Schistosoma* (n = 4), or Wilson's disease (n = 2), were excluded from the analysis, as
426 were samples from two pregnant women. In all, 1,534 samples from 9 studies were
427 downloaded from the sequence read archive (SRA) and further processed (Table S3)
428 for a total of 1,821 samples with at least one million sequence pairs per sample.

429 **Data processing** - A detailed description of the processing of the raw sequences
430 is given in Appendix 1. To obtain a taxonomic profile of the metagenome samples, we
431 built a custom genomes database (55) for Kraken v2.0.7 (56) and Bracken v2.2 (57)
432 using the representative genomes from the Progenomes database (as available on

433 August 24 2018) (58), to which we added genome sequences of *C. minuta* (GenBank
434 assembly accession: GCA_001652705.1), *C. massiliensis* (GCA_900155415.1), and *C.*
435 *timonensis* (GCA_900087015.1). Reads were classified using Kraken2 and a Bayesian
436 re-estimation of the species-level abundance of each sample was then performed using
437 Bracken2. We obtained complete taxonomic annotations from NCBI taxIDs with
438 TaxonKit v0.2.4 (<https://bioinf.shenwei.me/taxonkit/>). The detection limit for the relative
439 abundances in samples was 10^{-3} %; in consequence, all relative abundances below this
440 threshold were equal to 0.

441 **Meta-analysis of human gut metagenomes** - Linear mixed models (R package
442 nlme) were used to evaluate the correlation between the relative abundances of taxa
443 while correcting for the structure of the population; the study of origin was set as a
444 random effect. In some datasets, individuals were sampled multiple times in which case
445 the individual effect was nested inside the dataset effect. Relative abundances were
446 transformed using the Tukey's ladder of powers transformation (59), and are designated
447 with the suffix '-tra' (e.g., the transformed relative abundance of the family
448 *Christensenellaceae* is Cf-tra). Covariates in null models were selected using a
449 backward feature selection approach based on a type II ANOVA (i.e., by including all
450 covariates and removing the non-significant ones step-by-step until all remaining
451 variables were significant, Appendix 2). We made 4 null models predicting the
452 transformed relative abundance of the family *Christensenellaceae* (Cf-null), the genus
453 *Christensenella* (Cg-null), the family *Methanobacteriaceae* (Mf-null) and the genus
454 *Methanobrevibacter* (Mg-null). To evaluate the correlation between taxa, we made
455 model Cf-Mf by adding Mf-tra and its interaction with age to the covariates of Cf-null.

456 Reciprocally, we made model Cg-Mg by adding Mg-tra and its interaction with age to
457 the covariates of Cg-null. The same approach was performed at the species level and it
458 is described in Appendix 2.

459 (Cf-null) $Cf\text{-tra} = BMI + age + 1 \mid Dataset/Individual$

460 (Cg-null) $Cg\text{-tra} = BMI + age + 1 \mid Dataset/Individual$

461 (Mf-null) $Mf\text{-tra} = BMI + age + 1 \mid Dataset/Individual$

462 (Mg-null) $Mg\text{-tra} = BMI + age + 1 \mid Dataset/Individual$

463 (Cf-Mf) $Cf\text{-tra} = BMI + age + Mf\text{-tra} + age * Mf\text{-tra} +$

464 $1 \mid Dataset/Individual$

465 (Cg-Mg) $Cg\text{-tra} = BMI + age + Mg\text{-tra} + age * Mg\text{-tra} +$

466 $1 \mid Dataset/Individual$

467 We used the likelihood ratio test to compare the nested models via the χ^2
468 distribution (*i.e.* Cf-null vs. Cf-Mf and Cg-null vs. Cg-Mg). To characterize the correlation
469 of Cf-tra with Mf-tra, and Cg-tra with Mg-tra, after correcting for BMI and age, we used a
470 type I ANOVA to evaluate the importance of the variables in the order they appear in Cf-
471 Mf and Cg-Mg. The F-value, degree of freedom and p-value are reported for each
472 variable. All analyses were performed using R (60).

473 **Culturing of methanogens and bacteria** – We obtained *M. smithii* DSM-861, *C.*
474 *minuta* DSM-22607, *C. massiliensis* DSM 102344, *C. timonensis* DSM 102800, and *B.*
475 *thetaitaomicron* VPI-5482 from the German Collection of Microorganisms and Cell
476 Cultures (DSMZ; Braunschweig, Germany). Each culture was thawed and inoculated
477 into Brain Heart Infusion (BHI) medium (Carl Roth, Karlsruhe, Germany) supplemented
478 with yeast extract (5 g/L), reduced with L-Cysteine-HCl (0.5 g/L) and Ti-NTA III (0.3

479 mM), and buffered with sodium bicarbonate (42 mM, pH 7, adjusted with HCl 6M). 10
480 mL cultures were grown at 37°C without shaking in Balch tubes (total volume of 28 mL)
481 under a headspace of N₂:CO₂ (80:20% v/v) in the case of the bacteria, and H₂:CO₂
482 (80:20% v/v, pressure adjusted to 2 bar) for *M. smithii*. When initial cultures reached
483 exponential growth, and before floc formation, they were transferred into fresh medium
484 and these transfers were used as inocula for the experiments described below.

485 **Co-culture conditions** - *M. smithii* was co-cultured with *C. minuta*, *B.*
486 *thetaitaomicron*, *C. massiliensis*, or *C. timonensis*, and in parallel, each microorganism
487 was grown in mono-culture (Table S1). Prior to inoculation, one-day old cultures of
488 bacterial species, or 4-day old cultures of *M. smithii*, were adjusted to an OD₆₀₀ of 0.01
489 with sterile medium. For the co-cultures, 0.5 mL of each adjusted culture was inoculated
490 into 9 mL of fresh medium. For the mono-cultures, 0.5 mL of the adjusted culture and
491 0.5 mL of sterile medium were combined as inoculum. For negative controls, sterile
492 medium was transferred as a mock inoculum. Headspaces were exchanged with 80:20
493 % (v/v) of N₂:CO₂ or H₂:CO₂ and pressurized at 2 bar or atmospheric pressure (Table
494 S1). Each batch of experiments was carried out once with 3 biological replicates per
495 culture conditions (Table S1).

496 **Imaging** - For confocal microscopy, SYBR[®] Green I staining was performed as
497 previously described (61) with the modifications described in Appendix 1. Imaging by
498 confocal microscopy (LSM 780 NLO, Zeiss) was used to detect the autofluorescence
499 emission of coenzyme F₄₂₀ of *M. smithii* and the emission of SYBR Green I (Appendix
500 1). Images were acquired with the ZEN Black 2.3 SP1 software and processed with FIJI
501 (62). Micrographs are representative of all replicate cultures within each experimental

502 batch. The preparation of the samples for scanning electron microscopy is described in
503 Appendix 1. Cells were examined with a field emission scanning electron microscope
504 (Regulus 8230, Hitachi High Technologies, Tokyo, JPN) at an accelerating voltage of 10
505 kV.

506 **Gas and SCFA measurements** - Headspace concentrations of H₂, CO₂, and
507 CH₄ were measured with a gas chromatograph (GC) (SRI 8610C; SRI Instruments,
508 Torrence, USA) equipped with a packed column at 42 °C (0.3-m HaySep-D packed
509 Teflon; Restek, Bellefonte, USA), a thermal conductivity detector (TCD) at 111 °C, and a
510 flame ionization (FID) detector. The gas production and consumption were estimated
511 from the total pressure in the vials (ECO2 manometer; Keller, Jestetten, Germany) and
512 the gas concentrations in the headspace using the ideal gas equation. The
513 concentrations are given in mmol of gas in the headspace per liter of culture.

514 SCFA measurements were performed with liquid samples (0.5 mL) filtered
515 through 0.2 µm pore size polyvinylidene fluoride filters (Carl Roth, GmbH, Karlsruhe,
516 GER). SCFA concentrations were measured with a CBM-20A high performance liquid
517 chromatography (HPLC) system equipped with an Aminex HPX- 87P column (300 x 7.8
518 mm, BioRad, California, USA), maintained at 60 °C, and a refractive index detector. A
519 sulfuric acid solution (5 mM) was used as eluent at a flow rate of 0.6 mL/min (~40 bar
520 column pressure). Calibration curves for acetate and butyrate were prepared from 1.25
521 to 50 mM using acetic acid and butyric acid, respectively (Merck KGaA, Darmstadt,
522 Germany). No other fatty acids were detected (Appendix 1). The SCFA concentrations
523 were estimated with the Shimadzu LabSolutions software.

524 **Statistical analyses** - We used Wilcoxon rank sum tests to compare gas
525 production between cultures after 6 days of growth. We performed ANOVA tests when
526 more than one culture condition (*i.e.*, headspace composition and pressure, Table S1)
527 was included in the comparison. The conditions in the ANOVA tests (*i.e.*, headspace
528 composition and pressure, in mono- or co-culture) were evaluated to explain the
529 variance of CH₄ production after 6 days of growth. A Tukey's post-hoc test was then
530 performed to discriminate between the effects of the different conditions. SCFA
531 concentrations were compared using a two-way ANOVA where the culture conditions
532 (*i.e.*, headspace composition and pressure, Table S1) and the sample (mono- and co-
533 culture) were evaluated to explain the variance of butyrate and acetate concentrations
534 after 6 days of growth. p-values were adjusted using the Benjamini-Hochberg method. A
535 Tukey's post-hoc test was performed to discriminate between the effects of the different
536 conditions. All statistical analyses were done in R using the stats R package.

537 **Data and code availability** - The metagenomic sequence data generated during
538 this study have been deposited in the European Nucleotide Archive with accession IDs
539 PRJEB34191 (<http://www.ebi.ac.uk/ena/data/view/PRJEB34191>). The jupyter
540 notebooks and associated data are available at
541 https://github.com/Albabune/Ruaud_EsquivelElizondo.

542

543 **Acknowledgments**

544 We are grateful to Monika Temovska, Sophie Maisch and Iris Holdermann for
545 valuable help. We also thank Daren Heavens for the metagenome library preparation

546 protocol. This work was supported by the Max Planck Society and the Humboldt
547 Foundation.

548

549 **Appendixes**

550 **Appendix 1. Additional methods**

551 **Metagenomic libraries preparation** - Metagenomic libraries were prepared
552 using 1 ng of DNA input per sample (extracted with the MagAttract PowerSoil DNA kit,
553 Qiagen) as previously described (63). Fragment sizes were restricted to 400 - 700 bp
554 using BluePippin (Sage Science), and samples were pooled at equimolar
555 concentrations before being run on an Illumina HiSeq3000 with 2x150 bp paired end
556 sequencing, resulting in sequencing depths of 3.0 ± 2.1 Gb (median \pm standard
557 deviation).

558 **Raw Data processing** - Raw sequences were first validated using fqtools v.2.0 (64)
559 and de-duplicated with the “clumpify” command of bbtools v37.78
560 (<https://jgi.doe.gov/data-and-tools/bbtools/>). We trimmed adapters and performed read
561 quality control using skewer v0.2.2 (65) and the “bbduk” command of bbtools. We used
562 the “bbmap” command of bbtools to filter human genome reads that mapped to the
563 hg19 assembly. Finally, we generated QC reports for all reads with fastqc v0.11.7
564 (<https://github.com/s-andrews/FastQC>) and multiQC v1.5a (66).

565 **Confocal imaging, equipment, and settings** - For confocal microscopy, SYBR[®]
566 Green I staining was performed as previously described (61) with the following
567 modifications: 0.5 mL of culture were sampled and pelleted by centrifugation for 6 min at

568 6,000 xg (Benchtop centrifuge, Eppendorf, Hamburg, Germany) and pellets were
569 resuspended in a solution containing 744 μ L 1x PBS, 16 μ L 25x SYBR[®] Green I
570 (Sigma-Aldrich, Merck, Germany) and 40 μ L 70% v/v ethanol. Samples were pelleted
571 and resuspended before imaging in 100 μ L 1x PBS, of which 5 μ L were immobilized
572 on 50 μ L solid agar (1.5% noble agar in distilled water) (67). Imaging was performed
573 with a confocal microscope (LSM 780 NLO, Zeiss) using oil and water objectives (40x
574 and 63x). A DPSS laser at 405 nm was used to excite the F₄₂₀ enzyme of *M. smithii*.
575 Autofluorescence emission was collected on a 32 channel GaAsP array from 455 to 499
576 nm. A transmitted light detector (T-PMT) was used to collect the whole light spectrum to
577 create a bright field image. On a second track, an Argon laser at 488 nm was used to
578 excite SYBR[®] Green I and its emission was collected from 508 to 588 nm with the 32
579 channel GaAsP array as well. Images were acquired with a time and space resolution of
580 2048x2048x(1 to 12)x (xyzt) and pixel dimensions of 0.1038x0.1038 μ m for the images
581 taken with the x40 oil objective and pixel dimensions of 0.0659x0.0659 μ m for the
582 images taken with the x63 oil objective. The bit depth was 16-bit. Acquisition was
583 performed at 20 °C.

584 **Processing of the confocal images** - FIJI (62) was used to process the confocal
585 micrographs. Contrast and brightness adjustment were applied to the whole image. Due
586 to the thickness of the aggregates of *Christensenella minuta*, the SYBR[®] Green I
587 fluorescence intensity was varied with different focal planes. We used a gamma
588 transformation (with gamma = 0.50) to homogenize the fluorescence intensity. The
589 exact same transformation was applied to all samples, even though there were no
590 aggregates, for consistency purposes. Similarly, we applied a gamma transformation to

591 the F₄₂₀ autofluorescent channel to decrease the low fluorescence coming from SYBR[®]
592 Green I (gamma = 1.20 to 1.50). As their excitation and emission spectra overlap, there
593 was a low fluorescence intensity of the SYBR[®] Green I on the F₄₂₀ autofluorescent
594 channel. The lookup tables (LUT) were Cyan Hot for the F₄₂₀ autofluorescence and red
595 (linear LUT, covering the full range of the data) for the SYBR[®] Green I fluorescence.

596 **Preparation of samples for scanning electron microscopy** - Pellets were washed
597 3-5 times with 1x PBS and then fixed with a 2.5% v/v glutaraldehyde solution in 1x PBS
598 for 1-2 h at room temperature and post-fixed with 1% w/v osmium tetroxide for 1h on
599 ice. Samples were dehydrated in a graded ethanol series followed by drying with CO₂ in
600 a Polaron critical point dryer (Quorum Technologies, East Sussex, UK). Finally, cells
601 were sputter coated with a 5 nm thick layer of platinum (CCU-010 Compact coating unit,
602 Safematic GmbH, Bad Ragaz, SWI).

603 **Screening of the short and medium chain fatty acids produced** - Before carrying
604 out the experiments presented in the main text, we used gas chromatography (GC) to
605 determine which fatty acids were produced by the cultures and if the corresponding
606 peaks were present in BHI. For this screening, the external standards included
607 equimolar mixtures of acetate, propionate, iso-butyrate, butyrate, iso-valerate, valerate,
608 iso-caproate, caproate, heptanoate, and caprylate, from 0.2 to 7 mM. Measurements
609 were performed with a 7890B GC system (Agilent Technologies Inc., Santa Clara, USA)
610 equipped with a capillary column (DB-Fatwax UI 30 m x 0.25 m; Agilent Technologies)
611 and an FID detector with a ramp temperature program (initial temperature of 80 °C for
612 0.5 min, then 20 °C per min up to 180°, and final temperature of 180 °C for 1 min). The
613 injection and detector temperatures were 250 and 275 °C, respectively. Samples were

614 prepared as for HPLC (Methods in the main text) with the addition of an internal
615 standard (Ethyl-butyric acid) and acidification (to pH 2) with 50% formic acid. Data were
616 acquired and analysed with the Agilent OpenLAB CDS software.

617 Only acetate and butyrate were detected in the mono- and co-cultures, and none of
618 the other short and medium chain fatty acids used as standards were detected. As
619 formate was used to acidify samples for the GC measurements, to assess if it was a
620 main product in the cultures, its concentration was measured by HPLC. We also looked
621 for ethanol using HPLC but similar to formate, it was not detected in any of the
622 cultures. Thus, for the experiments in the main text, only acetate and butyrate were
623 quantified via HPLC. BHI medium showed peaks corresponding to 0.33 mM formate
624 and 6 mM of acetate, which were subtracted from the reported concentrations of the
625 cultures.

626

627 **Appendix 2. Additional statistics**

628 **Variable selection for the null model** - To construct the null model, we tested the
629 effect of the following covariates with a marginal ANOVA: sequencing depth, gender,
630 country, BMI, and age. The sequencing depth was not significant (p -value = 0.73) and
631 was subsequently removed. BMI and age were correlated with the *Chistensenellaceae*
632 abundance (p -value = 0.0002 for the correlation with BMI and 0.02 for the correlation
633 with age).

634 As *Methanobrevibacter smithii* has been associated with age (23) and BMI (4, 43,
635 45–48, 68, 69), we first added the interaction factors to the models: the interaction
636 factors were not significant with BMI (p -values = 0.11 and 0.07, for both

637 *Methanobrevibacter* and *Methanobacteriaceae*, respectively). However, the interactions
638 with age were significant (p-values = 0.004 and 0.002, for both *Methanobrevibacter* and
639 *Methanobacteriaceae*, respectively) and therefore, both variables were kept in the
640 models.

641 **Statistical analysis at the species rank** - Similar to the analysis at family and genus
642 levels presented in the main text, we performed an analysis at the species level
643 between *Christensenella minuta* and *Methanobrevibacter smithii*, the most abundant
644 and prevalent species of their genera. We also studied the correlation of the other two
645 known species of *Christensenella*, i.e., *C. massiliensis* and *C. timonensis*, with *M.*
646 *smithii*. *M. smithii* was detected in 78.7 % of the samples with a mean relative
647 abundance of 0.53 % (*M. oralis* was the only other *Methanobrevibacter* detected, with a
648 prevalence of 42.8 % and a mean relative abundance of 3.07×10^{-3} %). *C. minuta* had an
649 averaged relative abundance of 0.05% in the 99.7% samples where it was present. *C.*
650 *timonensis* and *C. massiliensis* had respectively, prevalences of 95.11 % and 98.57 %
651 and mean relative abundances of 6.49×10^{-3} % and 0.02 %.

652 *M. smithii* was significantly positively correlated with age (type II ANOVA, F-value =
653 13.22 and p-value = 2.86×10^{-4}) and negatively correlated with BMI (type II ANOVA, F-
654 value = 4.13 and p-value = 0.04). The association between *M. smithii* and leanness was
655 not as strong as for its family and genus levels, meaning that other
656 *Methanobacteriaceae* members must contribute to the strength of the association.

657 Consistently with the analyses at the family and genus levels, *Christensenella minuta*
658 and *Methanobrevibacter smithii* were significantly correlated (χ^2 test, p-value = $1.05 \times 10^{-$
659 ³⁴) and the effect of *M. smithii* was significant (type I ANOVA, p-value < 0.0001, F-value

660 = 147.82). Moreover, *C. minuta*'s relative abundance correlated with both age and BMI
661 (type I ANOVA, p-values = 0.0071 and 0.0011, F-values = 7.28 and 10.91,
662 respectively), as well as with the interaction term between *M. smithii* and age (type I
663 ANOVA, p-value < 0.0001, F-value = 17.99).

664 *Christensenella timonensis* and *M. smithii* were correlated (χ^2 test, p-value = 6.12×10^{-98} ;
665 type I ANOVA, p-value < 0.0001, F-value = 482.42). And, similar to *C. minuta*, the
666 relative abundance of *C. timonensis* correlated with both age and BMI (type I ANOVA,
667 p-values = 0.0012 and 0.0001, F-values = 10.59 and 16.61, respectively), as well as
668 with the interaction term between *M. smithii* and age (type I ANOVA, p-value < 0.0001,
669 F-value = 35.50).

670 The relative abundance of *Christensenella massiliensis* correlated with BMI (type I
671 ANOVA, p-value = 0.0028 and F-value = 9.0804) but not with age (p-value > 0.5) and
672 so, we did not correct for age in the null model nor in the model including
673 *Methanobrevibacter smithii*'s transformed relative abundance. *C. massiliensis* and *M.*
674 *smithii* were also correlated (χ^2 test, p-value = 1.31×10^{-61} ; type I ANOVA, p-value <
675 0.0001, F-value = 310.51), but the interaction term between *M. smithii* and age was not
676 significantly correlated to the bacterium's abundance. *C. massiliensis* is thus the only
677 *Christensenella* spp. for which the correlation with the methanogen abundance is not a
678 function of the age of the carrier.

679

680 **Appendix 3. Comparison of the expected (theoretical) vs. the measured methane**
681 **production in co-cultures**

682 We used the stoichiometry of hydrogenotrophic methanogenesis ($\text{CO}_2 + 4 \text{H}_2 = \text{CH}_4$
 683 $+ 2 \text{H}_2\text{O}$) to calculate the amount of CH_4 that could be produced from the estimated
 684 amount of H_2 consumed in each sample. For this, we used the mono-cultures of
 685 bacteria as references and assumed equal H_2 production in co-culture as in mono-
 686 culture. We estimated the H_2 consumed after 6 days for each replicate as the difference
 687 between the averaged H_2 concentrations in mono-cultures and the concentration
 688 measured in co-culture (*i.e.*, unconsumed H_2). The estimated H_2 consumed was then
 689 divided by 4 in order to obtain the theoretical amount of CH_4 that could be produced via
 690 hydrogenotrophic methanogenesis.

691
 692 **Table A3. Analysis of the origin of the high methane produced in co-culture**
 693 **based on the changes in metabolism of *C. minuta*.** CH_4 produced in co-culture was
 694 higher than the theoretical amount of CH_4 that could be generated from H_2 assuming
 695 that *C. minuta* produced the same amount of H_2 in both mono- and co-cultures. The
 696 additional CH_4 observed could originate from the shift in metabolism from butyrate to
 697 acetate production along with H_2 by *C. minuta* in co-culture. The average concentration
 698 among the triplicates after 6 days of growth is given with the standard deviation (SD).

Condition	$\text{H}_2:\text{CO}_2$ - 2 bar ^a		$\text{N}_2:\text{CO}_2$ - atm		$\text{N}_2:\text{CO}_2$ - 2 bar	
	Average	SD	Average	SD	Average	SD
H_2 produced in mono-culture (mmol.L^{-1})	18.71	9.71	17.28	1.12	14.15	1.56
H_2 not consumed in co-culture ^b (mmol.L^{-1})	-21.81	0.87	0.08	0.01	0.03	0.00
Theoretical CH_4 produced based on H_2 produced in mono-culture (mmol.L^{-1} ^c)	10.13	0.22	4.30	0.00	3.53	0.00

Observed CH ₄ produced in co-culture (mmol.L ⁻¹)	14.21	5.33	6.57	0.77	5.81	0.45
Difference between observed and theoretical CH ₄ (mmol.L ⁻¹)	04.08	5.50	2.27	0.77	2.28	0.45
Butyrate difference between co- and mono-culture (mmol.L ⁻¹)	-1.11	0.30	-1.21	0.04	-0.91	0.27
Acetate difference between co- and mono-culture (mmol.L ⁻¹)	0.68	0.10	2.20	0.22	1.36	0.17

699

700 ^a For the experiments grown under an H₂:CO₂ (80:20 %) atmosphere, the average H₂ concentration

701 measured in the negative controls after 6 days (sampled as many times as the cultures) was subtracted

702 from the concentration measured in the cultures.

703 ^b Average of the concentration of H₂ in co-cultures to which the average of H₂ concentration in mono-

704 culture of *C. minuta* was subtracted.

705 ^c This amount is calculated based on the stoichiometry of the hydrogenotrophic methanogenesis reaction:

706 $4 \text{ H}_2 + \text{CO}_2 = \text{CH}_4 + 2 \text{ H}_2\text{O}$.

707 **References**

- 708 1. Ley RE, Turnbaugh PJ, Klein S, Gordon JI. 2006. Microbial ecology: Human gut microbes
709 associated with obesity. *Nature* 444:1022–1023.
- 710 2. Turnbaugh PJ, Ley RE, Mahowald MA, Magrini V, Mardis ER, Gordon JI. 2006. An obesity-
711 associated gut microbiome with increased capacity for energy harvest. *Nature* 444:1027–
712 1031.
- 713 3. Waters JL, Ley RE. 2019. The human gut bacteria *Christensenellaceae* are widespread,
714 heritable, and associated with health. *BMC Biol* 17:83.
- 715 4. Goodrich JK, Waters JL, Poole AC, Sutter JL, Koren O, Blekhman R, Beaumont M, Van
716 Treuren W, Knight R, Bell JT, Spector TD, Clark AG, Ley RE. 2014. Human genetics shape
717 the gut microbiome. *Cell* 159: 789–799.
- 718 5. Fu J, Bonder MJ, Cenit MC, Tigchelaar EF, Maatman A, Dekens JAM, Brandsma E,
719 Marczynska J, Imhann F, Weersma RK, Franke L, Poon TW, Xavier RJ, Gevers D, Hofker
720 MH, Wijmenga C, Zhernakova A. 2015. The gut microbiome contributes to a substantial
721 proportion of the variation in blood lipids. *Circ Res* 117:817–824.
- 722 6. Goodrich JK, Davenport ER, Beaumont M, Jackson MA, Knight R, Ober C, Spector TD,
723 Bell JT, Clark AG, Ley RE. 2016. Genetic determinants of the gut microbiome in UK Twins.
724 *Cell Host Microbe* 19:731–743.
- 725 7. Kummen M, Holm K, Anmarkrud JA, Nygård S, Vesterhus M, Høivik ML, Trøseid M,
726 Marschall H-U, Schrupf E, Moum B, Røsjø H, Aukrust P, Karlsen TH, Hov JR. 2016. The
727 gut microbial profile in patients with primary sclerosing cholangitis is distinct from patients
728 with ulcerative colitis without biliary disease and healthy controls. *Gut* 66:611–619.

- 729 8. Lim MY, You HJ, Yoon HS, Kwon B, Lee JY, Lee S, Song Y-M, Lee K, Sung J, Ko G. 2016.
730 The effect of heritability and host genetics on the gut microbiota and metabolic syndrome.
731 Gut 66:1031-1038.
- 732 9. Oki K, Toyama M, Banno T, Chonan O, Benno Y, Watanabe K. 2016. Comprehensive
733 analysis of the fecal microbiota of healthy Japanese adults reveals a new bacterial lineage
734 associated with a phenotype characterized by a high frequency of bowel movements and a
735 lean body type. BMC Microbiol 16:284.
- 736 10. Stanislowski MA, Dabelea D, Wagner BD, Sontag MK, Lozupone CA, Eggesbø M. 2017.
737 Pre-pregnancy weight, gestational weight gain, and the gut microbiota of mothers and their
738 infants. Microbiome 5:113.
- 739 11. Yun Y, Kim H-N, Kim SE, Heo SG, Chang Y, Ryu S, Shin H, Kim H-L. 2017. Comparative
740 analysis of gut microbiota associated with body mass index in a large Korean cohort. BMC
741 Microbiol 17:151.
- 742 12. Brooks AW, Priya S, Blekhman R, Bordenstein SR. 2018. Gut microbiota diversity across
743 ethnicities in the United States. PLoS Biol 16:e2006842.
- 744 13. Jackson MA, Bonder MJ, Kuncheva Z, Zierer J, Fu J, Kurilshikov A, Wijmenga C,
745 Zhernakova A, Bell JT, Spector TD, Steves CJ. 2018. Detection of stable community
746 structures within gut microbiota co-occurrence networks from different human populations.
747 PeerJ 6:e4303.
- 748 14. López-Contreras BE, Morán-Ramos S, Villarruel-Vázquez R, Macías-Kauffer L, Villamil-
749 Ramírez H, León-Mimila P, Vega-Badillo J, Sánchez-Muñoz F, Llanos-Moreno LE,
750 Canizalez-Román A, Del Río-Navarro B, Ibarra-González I, Vela-Amieva M, Villarreal-
751 Molina T, Ochoa-Leyva A, Aguilar-Salinas CA, Canizales-Quinteros S. 2018. Composition

- 752 of gut microbiota in obese and normal-weight Mexican school-age children and its
753 association with metabolic traits. *Pediatr Obes* 13:381–388.
- 754 15. Peters BA, Shapiro JA, Church TR, Miller G, Trinh-Shevrin C, Yuen E, Friedlander C,
755 Hayes RB, Ahn J. 2018. A taxonomic signature of obesity in a large study of American
756 adults. *Sci Rep* 8:9749.
- 757 16. Morotomi M, Nagai F, Watanabe Y. 2012. Description of *Christensenella minuta* gen. nov.,
758 sp. nov., isolated from human faeces, which forms a distinct branch in the order
759 *Clostridiales*, and proposal of *Christensenellaceae* fam. nov. *Int J Syst Evol Microbiol*
760 62:144–149.
- 761 17. Costea PI, Hildebrand F, Arumugam M, Bäckhed F, Blaser MJ, Bushman FD, Vos WM de,
762 Ehrlich SD, Fraser CM, Hattori M, Huttenhower C, Jeffery IB, Knights D, Lewis JD, Ley RE,
763 Ochman H, O'Toole PW, Quince C, Relman DA, Shanahan F, Sunagawa S, Wang J,
764 Weinstock GM, Wu GD, Zeller G, Zhao L, Raes J, Knight R, Bork P. 2018. Enterotypes in
765 the landscape of gut microbial community composition. *Nature Microbiology* 3:8–16.
- 766 18. Turpin W, Espin-Garcia O, Xu W, Silverberg MS, Kevans D, Smith MI, Guttman DS,
767 Griffiths A, Panaccione R, Otley A, Xu L, Shestopaloff K, Moreno-Hagelsieb G, GEM
768 Project Research Consortium, Paterson AD, Croitoru K. 2016. Association of host genome
769 with intestinal microbial composition in a large healthy cohort. *Nat Genet* 48:1413–1417.
- 770 19. Bonder MJ, Kurilshikov A, Tigchelaar EF, Mujagic Z, Imhann F, Vila AV, Deelen P, Vatanen
771 T, Schirmer M, Smeekens SP, Zhernakova DV, Jankipersadsing SA, Jaeger M, Oosting M,
772 Cenit MC, Masclee AAM, Swertz MA, Li Y, Kumar V, Joosten L, Harmsen H, Weersma RK,
773 Franke L, Hofker MH, Xavier RJ, Jonkers D, Netea MG, Wijmenga C, Fu J, Zhernakova A.
774 2016. The effect of host genetics on the gut microbiome. *Nat Genet* 48:1407–1412.

- 775 20. Hansen EE, Lozupone CA, Rey FE, Wu M, Guruge JL, Narra A, Goodfellow J, Zaneveld
776 JR, McDonald DT, Goodrich JA, Heath AC, Knight R, Gordon JI. 2011. Pan-genome of the
777 dominant human gut-associated archaeon, *Methanobrevibacter smithii*, studied in twins.
778 Proc Natl Acad Sci USA 108 Suppl 1:4599–4606.
- 779 21. Upadhyaya B, McCormack L, Fardin-Kia AR, Juenemann R, Nichenametla S, Clapper J,
780 Specker B, Dey M. 2016. Impact of dietary resistant starch type 4 on human gut microbiota
781 and immunometabolic functions. Sci Rep 6:28797.
- 782 22. Klimenko NS, Tyakht AV, Popenko AS, Vasiliev AS, Altukhov IA, Ischenko DS, Shashkova
783 TI, Efimova DA, Nikogosov DA, Osipenko DA, Musienko SV, Selezneva KS, Baranova A,
784 Kuriilshikov AM, Toshchakov SM, Korzhenkov AA, Samarov NI, Shevchenko MA, Tepliuk
785 AV, Alexeev DG. 2018. Microbiome responses to an uncontrolled short-term diet
786 intervention in the frame of the citizen science project. Nutrients 10:576.
- 787 23. Vanderhaeghen S, Lacroix C, Schwab C. 2015. Methanogen communities in stools of
788 humans of different age and health status and co-occurrence with bacteria. FEMS Microbiol
789 Lett 362:fnv092.
- 790 24. Moore WEC, Johnson JL, Holdeman LV. 1976. Emendation of *Bacteroidaceae* and
791 *Butyrivibrio* and descriptions of *Desulfomonas* gen. nov. and ten new species in the genera
792 *Desulfomonas*, *Butyrivibrio*, *Eubacterium*, *Clostridium*, and *Ruminococcus*. Int J Syst Evol
793 Microbiol 26:238–252.
- 794 25. Traore SI, Khelaifia S, Armstrong N, Lagier JC, Raoult D. 2019. Isolation and culture of
795 *Methanobrevibacter smithii* by co-culture with hydrogen-producing bacteria on agar plates.
796 Clinical Microbiology and Infection 25:1561.e1–1561.e5.
- 797 26. Khelaifia S, Lagier J-C, Nkamga VD, Guilhot E, Drancourt M, Raoult D. 2016. Aerobic

- 798 culture of methanogenic archaea without an external source of hydrogen. *Eur J Clin*
799 *Microbiol Infect Dis* 35:985–991.
- 800 27. Nkamga VD, Lotte R, Roger P-M, Drancourt M, Ruimy R. 2016. *Methanobrevibacter smithii*
801 and *Bacteroides thetaiotaomicron* cultivated from a chronic paravertebral muscle abscess.
802 *Clin Microbiol Infect* 22:1008–1009.
- 803 28. Lau SKP, McNabb A, Woo GKS, Hoang L, Fung AMY, Chung LMW, Woo PCY, Yuen K-Y.
804 2007. *Catabacter hongkongensis* gen. nov., sp. nov., isolated from blood cultures of
805 patients from Hong Kong and Canada. *J Clin Microbiol* 45:395–401.
- 806 29. Rosa BA, Hallsworth-Pepin K, Martin J, Wollam A, Mitreva M. 2017. Genome sequence of
807 *Christensenella minuta* DSM 22607T. *Genome Announc* 5:e01451-16.
- 808 30. Hillmann B, Al-Ghalith GA, Shields-Cutler RR, Zhu Q, Gohl DM, Beckman KB, Knight R,
809 Knights D. 2018. Evaluating the information content of shallow shotgun metagenomics.
810 *mSystems* 3:e00069-18.
- 811 31. Gill SR, Pop M, Deboy RT, Eckburg PB, Turnbaugh PJ, Samuel BS, Gordon JI, Relman
812 DA, Fraser-Liggett CM, Nelson KE. 2006. Metagenomic analysis of the human distal gut
813 microbiome. *Science* 312:1355–1359.
- 814 32. Dridi B, Raoult D, Drancourt M. 2011. Archaea as emerging organisms in complex human
815 microbiomes. *Anaerobe* 17:56–63.
- 816 33. Edwards T, McBride BC. 1975. Biosynthesis and degradation of methylmercury in human
817 faeces. *Nature* 253:463–464.
- 818 34. Balch WE, Wolfe RS. 1976. New approach to the cultivation of methanogenic bacteria: 2-
819 mercaptoethanesulfonic acid (HS-CoM)-dependent growth of *Methanobacterium*

- 820 *ruminantium* in a pressurized atmosphere. Appl Environ Microbiol 32:781–791.
- 821 35. Stams AJM, Plugge CM. 2009. Electron transfer in syntrophic communities of anaerobic
822 bacteria and archaea. Nat Rev Microbiol 7:568–577.
- 823 36. Shen L, Zhao Q, Wu X, Li X, Li Q, Wang Y. 2015. Interspecies electron transfer in
824 syntrophic methanogenic consortia: From cultures to bioreactors. Renewable Sustainable
825 Energy Rev 54:1358–1367.
- 826 37. Angenent LT, Karim K, Al-Dahhan MH, Wrenn BA, Domínguez-Espinosa R. 2004.
827 Production of bioenergy and biochemicals from industrial and agricultural wastewater.
828 Trends Biotechnol 22:477–485.
- 829 38. Macfarlane S, Macfarlane GT. 2003. Regulation of short-chain fatty acid production. Proc
830 Nutr Soc 62:67–72.
- 831 39. Liu Y, Whitman WB. 2008. Metabolic, phylogenetic, and ecological diversity of the
832 methanogenic *Archaea*. Ann N Y Acad Sci 1125:171–189.
- 833 40. den Besten G, van Eunen K, Groen AK, Venema K, Reijngoud D-J, Bakker BM. 2013. The
834 role of short-chain fatty acids in the interplay between diet, gut microbiota, and host energy
835 metabolism. J Lipid Res 54:2325–2340.
- 836 41. Louis P, Flint HJ. 2017. Formation of propionate and butyrate by the human colonic
837 microbiota. Environ Microbiol 19:29–41.
- 838 42. Hoyles L, Swann J. 2019. Influence of the human gut microbiome on the metabolic
839 phenotype, p. 535–560. In Lindon, JC, Nicholson, JK, Holmes, E (eds.), The Handbook of
840 Metabolic Phenotyping. Elsevier.
- 841 43. Mbakwa CA, Penders J, Savelkoul PH, Thijs C, Dagnelie PC, Mommers M, Arts ICW.

- 842 2015. Gut colonization with *Methanobrevibacter smithii* is associated with childhood weight
843 development. *Obesity* 23:2508–2516.
- 844 44. Morrison DJ, Preston T. 2016. Formation of short chain fatty acids by the gut microbiota
845 and their impact on human metabolism. *Gut Microbes* 7:189–200.
- 846 45. Mack I, Cuntz U, Grämer C, Niedermaier S, Pohl C, Schwartz A, Zimmermann K, Zipfel S,
847 Enck P, Penders J. 2016. Weight gain in anorexia nervosa does not ameliorate the faecal
848 microbiota, branched chain fatty acid profiles, and gastrointestinal complaints. *Sci Rep*
849 6:26752.
- 850 46. Armougom F, Henry M, Vialettes B, Raccach D, Raoult D. 2009. Monitoring bacterial
851 community of human gut microbiota reveals an increase in *Lactobacillus* in obese patients
852 and methanogens in anorexic patients. *PLoS One* 4:e7125.
- 853 47. Million M, Maraninchi M, Henry M, Armougom F, Richet H, Carrieri P, Valero R, Raccach D,
854 Vialettes B, Raoult D. 2012. Obesity-associated gut microbiota is enriched in *Lactobacillus*
855 *reuteri* and depleted in *Bifidobacterium animalis* and *Methanobrevibacter smithii*. *Int J Obes*
856 36:817–825.
- 857 48. Schwartz A, Taras D, Schäfer K, Beijer S, Bos NA, Donus C, Hardt PD. 2010. Microbiota
858 and SCFA in lean and overweight healthy subjects. *Obesity* 18:190–195.
- 859 49. Blaxter KL, Clapperton JL. 1965. Prediction of the amount of methane produced by
860 ruminants. *Br J Nutr* 19:511–522.
- 861 50. Crutzen PJ, Aselmann I, Seiler W. 1986. Methane production by domestic animals, wild
862 ruminants, other herbivorous fauna, and humans. *Tellus B*, 38B: 271-284.
- 863 51. Callaway TR, Edrington TS, Rychlik JL, Genovese KJ, Poole TL, Jung YS, Bischoff KM,

- 864 Anderson RC, Nisbet DJ. 2003. Ionophores: their use as ruminant growth promotants and
865 impact on food safety. *Curr Issues Intest Microbiol* 4:43–51.
- 866 52. Kruger Ben Shabat S, Sasson G, Doron-Faigenboim A, Durman T, Yaacoby S, Berg Miller
867 ME, White BA, Shterzer N, Mizrahi I. 2016. Specific microbiome-dependent mechanisms
868 underlie the energy harvest efficiency of ruminants. *ISME J* 10:2958–2972.
- 869 53. Poole AC, Goodrich JK, Youngblut ND, Luque GG, Ruaud A, Sutter JL, Waters JL, Shi Q,
870 El-Hadidi M, Johnson LM, Bar HY, Huson DH, Booth JG, Ley RE. 2019. Human Salivary
871 Amylase Gene Copy Number Impacts Oral and Gut Microbiomes. *Cell Host Microbe*
872 25:553–564.e7.
- 873 54. Pasolli E, Schiffer L, Manghi P, Renson A, Obenchain V, Truong DT, Beghini F, Malik F,
874 Ramos M, Dowd JB, Huttenhower C, Morgan M, Segata N, Waldron L. 2017. Accessible,
875 curated metagenomic data through ExperimentHub. *Nat Methods* 14:1023.
- 876 55. de la Cuesta-Zuluaga J, Ley RE, Youngblut ND. 2019. Struo: a pipeline for building custom
877 databases for common metagenome profilers. *Bioinformatics*, btz899.
- 878 56. Wood DE, Salzberg SL. 2014. Kraken: ultrafast metagenomic sequence classification using
879 exact alignments. *Genome Biol* 15:R46.
- 880 57. Lu J, Breitwieser FP, Thielen P, Salzberg SL. 2017. Bracken: estimating species
881 abundance in metagenomics data. *PeerJ Computer Science* 3:e104.
- 882 58. Mende DR, Letunic I, Huerta-Cepas J, Li SS, Forslund K, Sunagawa S, Bork P. 2017.
883 proGenomes: a resource for consistent functional and taxonomic annotations of prokaryotic
884 genomes. *Nucleic Acids Res* 45:D529–D534.
- 885 59. Mangiafico SS. 2016. Summary and Analysis of Extension Program Evaluation in R,

- 886 version 1.15.0.
- 887 60. R Core Team. 2017. R: A language and environment for statistical computing. R
888 Foundation for Statistical Computing, Vienna, Austria.
- 889 61. Lambrecht J, Cichocki N, Hübschmann T, Koch C, Harms H, Müller S. 2017. Flow
890 cytometric quantification, sorting and sequencing of methanogenic archaea based on F₄₂₀
891 autofluorescence. *Microb Cell Fact* 16:180.
- 892 62. Schindelin J, Arganda-Carreras I, Frise E, Kaynig V, Longair M, Pietzsch T, Preibisch S,
893 Rueden C, Saalfeld S, Schmid B, Tinevez J-Y, White DJ, Hartenstein V, Eliceiri K,
894 Tomancak P, Cardona A. 2012. Fiji: an open-source platform for biological-image analysis.
895 *Nat Methods* 9:676–682.
- 896 63. Karasov TL, Almario J, Friedemann C, Ding W, Giolai M, Heavens D, Kersten S, Lundberg
897 DS, Neumann M, Regalado J, Neher RA, Kemen E, Weigel D. 2018. *Arabidopsis thaliana*
898 and *Pseudomonas* Pathogens Exhibit Stable Associations over Evolutionary Timescales.
899 *Cell Host Microbe* 24:168–179.e4.
- 900 64. Droop AP. 2016. fqtools: an efficient software suite for modern FASTQ file manipulation.
901 *Bioinformatics* 32:1883–1884.
- 902 65. Jiang H, Lei R, Ding S-W, Zhu S. 2014. Skewer: a fast and accurate adapter trimmer for
903 next-generation sequencing paired-end reads. *BMC Bioinformatics* 15:182.
- 904 66. Ewels P, Magnusson M, Lundin S, Käller M. 2016. MultiQC: summarize analysis results for
905 multiple tools and samples in a single report. *Bioinformatics* 32:3047–3048.
- 906 67. Garcia-Betancur JC, Yepes A, Schneider J, Lopez D. 2012. Single-cell Analysis of *Bacillus*
907 *subtilis* Biofilms Using Fluorescence Microscopy and Flow Cytometry. *J Vis Exp* 1–8.

- 908 68. Zhang H, DiBaise JK, Zuccolo A, Kudrna D, Braidotti M, Yu Y, Parameswaran P, Crowell
909 MD, Wing R, Rittmann BE, Krajmalnik-Brown R. 2009. Human gut microbiota in obesity and
910 after gastric bypass. *Proc Natl Acad Sci U S A* 106:2365–2370.
- 911 69. Turnbaugh PJ, Hamady M, Yatsunenko T, Cantarel BL, Duncan A, Ley RE, Sogin ML,
912 Jones WJ, Roe BA, Affourtit JP, Egholm M, Henrissat B, Heath AC, Knight R, Gordon JI.
913 2009. A core gut microbiome in obese and lean twins. *Nature* 457: 480–484.
- 914

915 **Figure Legends**

916 **Fig. 1. Abundances of the *Methanobacteriaceae* and *Christensenellaceae***
917 **families across populations.** (a) Countries where the human gut metagenomes used
918 in our meta-analysis (n = 1,821 samples) were recruited by 10 independent studies
919 (summarized in Dataset); (b) association between the transformed relative abundances
920 of *Christensenellaceae* and *Methanobacteriaceae*, in samples where the
921 *Methanobacteriaceae* was detected; (c) Number of samples for which the
922 *Methanobacteriaceae* were detected; d-e and f-g: same as b-c, at the genus and
923 species level respectively. The correlation between the transformed relative
924 abundances of both taxa at each taxonomic level was evaluated using linear mixed
925 models to corrected for covariates (ANOVA, p-values < 0.0001).

926

927 **Fig. 2. Confocal micrographs of the cultures at 3 days of growth.** Confocal
928 micrographs after 3 days of growth. (a) *C. minuta* alone; (b) *M. smithii* alone; (c) *B.*
929 *thetaitaomicron* alone; d: *M. smithii* and *C. minuta* together; and e: *M. smithii* and *B.*
930 *thetaitaomicron* together. SYBR Green I fluorescence (DNA staining) is shown in red
931 and *M. smithii*'s coenzyme F₄₂₀ autofluorescence is shown in blue. Scale bars represent
932 10 µm. Based on gases production, at 3 days of growth, *B. thetaitaomicron* was
933 already at stationary phase (explaining the elongated cells, see Fig. S2 for confocal
934 micrographs of *B. thetaitaomicron* and *M. smithii* at 2 days of growth), *C. minuta* was
935 at the end of the exponential phase and *M. smithii* was still in exponential phase.

936

937 **Fig. 3. Scanning electron micrographs of the cultures at 3-7 days of growth.**

938 (a, d, g and k) Representative Balch tubes of cultures of *C. minuta* (Cm), *M. smithii*
939 (Ms), *C. minuta* and *M. smithii* (Cm/Ms), and *B. thetaiotaomicron* and *M. smithii* (Bt/Ms)
940 after 7 days of growth. In panel g, the floc formed by Cm/Ms is indicated with an arrow.
941 (b-c) Scanning electron micrographs (SEMs) of mono-cultures of *C. minuta* at 5 days of
942 growth; (e-f) SEMs of mono-cultures *M. smithii* at 5 days of growth; (h-j) SEMs of co-
943 cultures of *C. minuta* and *M. smithii* at 7, 5 and 2 days of growth respectively; (l-n)
944 SEMs of co-cultures of *B. thetaiotaomicron* and *M. smithii* at 7 days of growth. Arrows
945 indicate *M. smithii* cells. Metal bars on panels a, d and j are from the tube rack.

946

947 **Fig. 4. Gas concentrations over time in mono- and co-cultures of *C. minuta*,**

948 ***B. thetaiotaomicron*, and *M. smithii* grown under different conditions.** (a-e) H₂

949 (orange) and CH₄ (blue) concentrations in the headspace over time in cultures from

950 batches 1-3 (see Table S1). Points represent the average of the 3 biological replicates

951 for each condition, and red bars join the minimal and maximal values. In conditions

952 where H₂ was provided in excess (H₂ - 2 bar and H₂ - atm, headspace initially

953 composed of 80:20 % H₂:CO₂), its concentrations are not shown for scale reasons.

954 Initial concentrations of H₂ in conditions where it was not provided in the headspace

955 were undetectable (N₂ - 2 bar and N₂ - atm, headspace initially composed of 80:20 %

956 N₂:CO₂) and stayed null in the mono-cultures of *M. smithii* (not shown). CH₄

957 concentrations in the bacterial mono-cultures were undetectable and are not shown as

958 well. Panels a-c share the same y-scale, as do panels d-e.

959

960 **Fig. 5. Summary of gases and SCFA produced in mono- and co-cultures of**
961 ***C. minuta*, *C. timonensis*, *C. massiliensis*, *B. thetaiotaomicron*, and *M. smithii***
962 **after 6 days of growth.** (a-d) H₂, CH₄, butyrate, and acetate production after 6 days of
963 growth in all mono- and co-cultures presented in this study (batches 1-4, Table S1).
964 Points represent the concentration of each biological replicate; (e) Table summarizing
965 the conditions for each culture. The conditions include the gas mixture (H₂:CO₂ or
966 N₂:CO₂ 80:20 % v/v), the initial pressure (2 bar or atmospheric) and the microorganisms
967 inoculated. C: *C. minuta*. Ct: *C. timonensis*. Cm: *C. massiliensis* (Cm). B: *B.*
968 *thetaiotaomicron*. M: *M. smithii*. Samples inoculated with the same microorganisms are
969 the same color.

970

971 **Fig. 6. SCFA concentrations over time in mono- and co-cultures of *C.***
972 ***minuta* and *M. smithii* grown under different conditions.** Short chain fatty acids over
973 time in cultures from batches 1-3 (see Table S1). (a-c) butyrate concentrations; d-f:
974 acetate concentrations. Only these SCFA were detected among the fatty acids tested
975 (fatty acids from C₁ to C₈, iso-valerate and iso-butyrate). Points represent the average of
976 the 3 biological replicates for each condition, and red bars join the minimal and maximal
977 values. Mono-cultures of *M. smithii* are not shown as they did not differ from the blanks
978 (negative controls).

979

980 **Fig. 7. Confocal imaging of *C. massiliensis* and *C. timonensis* in mono- and**
981 **co-cultures with *M. smithii*.** Confocal micrographs after 5 days of growth of (a) *C.*
982 *massiliensis*, (b) *M. smithii* and *C. massiliensis* in co-culture, (c) *C. timonensis*, d-e: *M.*

983 *smithii* and *C. timonensis* in co-culture. SYBR Green I fluorescence (DNA staining) is
984 shown in red and, *M. smithii*'s coenzyme F420 autofluorescence is shown in blue. Scale
985 bars represent 10 μm .

986

987 **Fig. 8. Gas and SCFA concentrations in mono- and co-cultures of *C.***

988 ***massiliensis* and *C. timonensis* with *M. smithii*.** (a-e) H₂ (orange) and CH₄ (blue)
989 concentrations in the headspace in cultures from batch 4 (see Table S1); (f-g) butyrate
990 and (h-i) acetate concentrations in these cultures. Points represent the average of 3
991 biological replicates, and red bars join the minimal and maximal values. In the mono-
992 cultures of *M. smithii* (b) where H₂ was provided in excess (condition H₂ - atm,
993 headspace initially composed of 80:20 % H₂:CO₂), its concentrations are not shown for
994 scale reasons.

995

996 **Fig. S1. Abundances of the *Methanobacteriaceae* and *Christensenellaceae***

997 **families across studies.** (a-j) Transformed relative abundances of *Christensenellaceae*
998 (*Cf-tra*) and *Methanobacteriaceae* (*Mf-tra*) across 1,821 samples from 10 countries and
999 generated from 10 independent studies. The data generated for this study are grouped
1000 with the first time series published in Poole et al., 2019. The gap between 0 and ~0.2 is
1001 due to the detection limit of the sequencing method; the minimal relative abundance is
1002 10⁻³ %. Hence, 0 indicates the microorganism was not detected, which introduces a gap
1003 after transformation of the data.

1004

1005 **Fig. S2. Confocal imaging of co-cultures of *B. thetaiotaomicron* and *M.***
1006 ***smithii* at different time points.** (a-b) cells at day 2, when *B. thetaiotaomicron* enters
1007 stationary phase (see Fig. 4d). (c-d) at day 7, the end of the experiment, when maximal
1008 CH₄ concentrations were observed both in mono-cultures of *M. smithii* and in co-
1009 cultures with *B. thetaiotaomicron* (Fig. 4b,e). In exponential phase, *B. thetaiotaomicron*
1010 cells are rod-shaped (a); while during stationary phase they suffer stress, leading to
1011 elongated cells (c). The bright fields (a and c) and *M. smithii*'s co-enzyme F₄₂₀ (b and d)
1012 channels are displayed. Scale bars represent 10 μm.

1013
1014 **Fig. S3. *C. minuta* and *M. smithii* also aggregate at atmospheric pressure**
1015 **and even when there is excess H₂ in the medium.** Confocal imaging of *C. minuta* and
1016 *M. smithii* at 3 days of growth. (a-b) co-culture grown at atmospheric pressure; (c-d) co-
1017 culture grown under a pressurized H₂:CO₂ atmosphere. The bright fields (a and c) and
1018 *M. smithii*'s co-enzyme F₄₂₀ (b and d) channels are displayed. Scale bars represent 10
1019 μm.

1020
1021 **Fig. S4. Additional batches.** H₂, CH₄, acetate, and butyrate concentrations in
1022 mono- and co-cultures of *M. smithii* and *C. minuta* grown at 2 bars, as described in the
1023 main text. The SCFA of batch S1 were measured by Gas Chromatography instead of
1024 High-Performance Liquid Chromatography. The points represent the average of 2 to 3
1025 biological cultures, and red bars join the minimal and maximal values.

1026

1027 **Tables**

1028 **Table S1. Total pressure, headspace composition, and culture inocula for**
1029 **each batch of experiments described in the main text.**

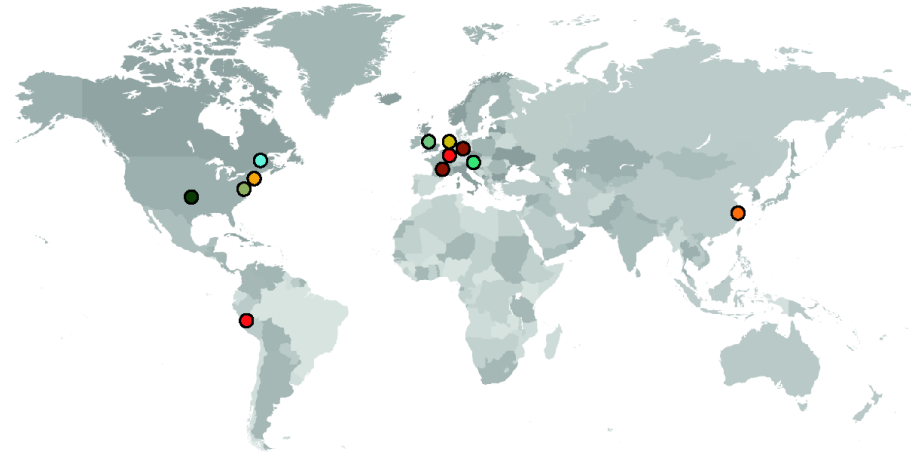
1030

1031 **Table S2. Samples from the Poole et al. (2019) study.** Additional data were
1032 generated from time points that had not been sequenced for the Poole et al. study. For
1033 each individual and each time point, the color indicates whether the sample was
1034 prepared and sequenced as previously (orange) or as described in the Methods (blue).
1035 If the sample was failed sequencing or was otherwise missing, the color is white.

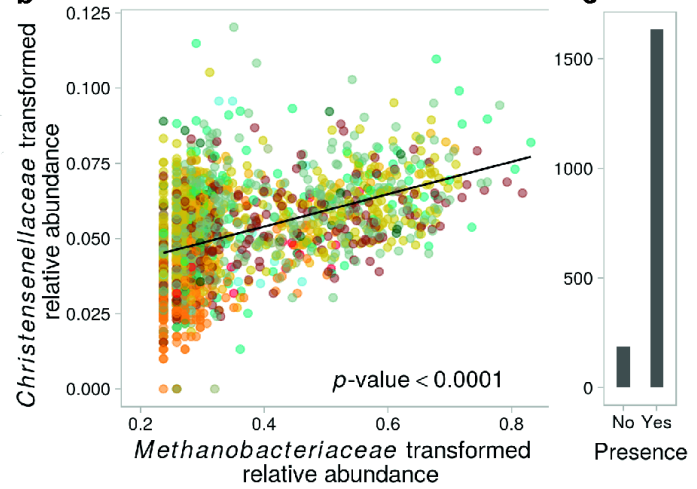
1036

1037 **Table S3. Datasets used for the statistical analysis.** The body mass index
1038 (BMI) and age values for each dataset are reported as an average value with minimum
1039 and maximum values in parentheses.

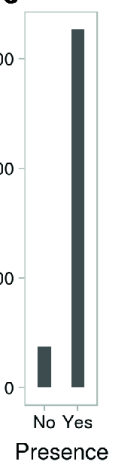
a



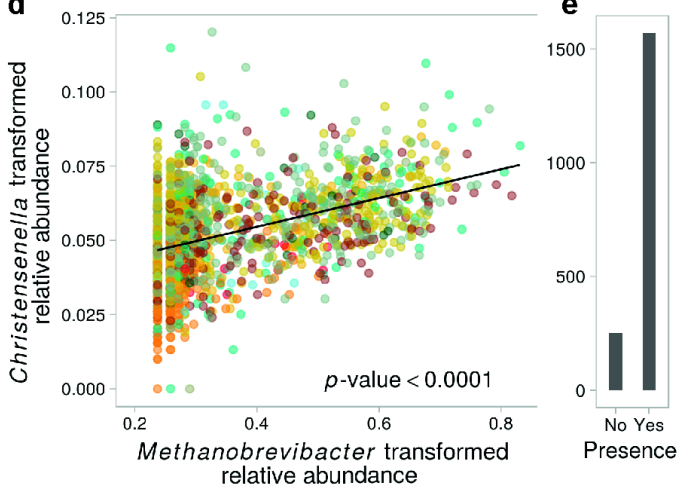
b



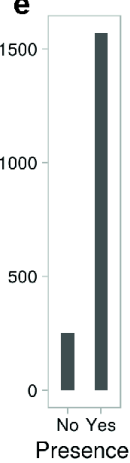
c



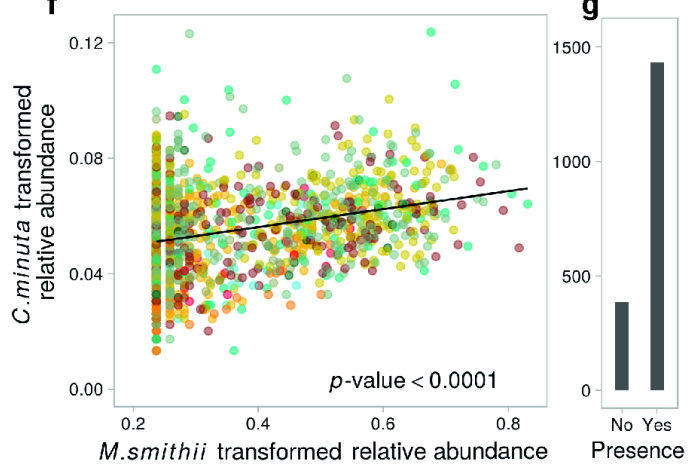
d



e



f



g



Dataset:

- BuschartA_2016
- FengQ_2015
- PooleA_2019
- QinN_2014
- RaymondF_2016
- SchirmerM_2016
- TitoAJ_2015
- VogtmannE_2016
- XieG_2016
- ZellerG_2014

